Proceedings of the Sustainable Research and Innovation Conference
JKUAT Main Campus, Kenya
6 - 7 October, 2021

Concurrent Sidelobe Minimization and Node Transmission Power Reduction in Collaborative Beamforming in Wireless Sensor Networks

Mr. Robert Macharia Maina and Dr. Kibet Lang'at and Dr. P. K. Kihato

Abstract—Collaborative Beamforming (CBF) is an essential tool towards increasing transmission range in Wireless Sensor Networks (WSNs). Conventional CBF (essentially beamsteering) is intricately associated with high sidelobes owing to the usual random WSN node arrangement. In WSNs high sidelobes imply increased interference at co-channel data sinks. This necessitates adoption of sidelobe minimization procedures in CBF. Also, WSN sensor nodes bear limited energy resources necessitating apt power control during CBF. Current literature focuses on peak sidelobe minimization upon conventional beamsteering; This yields sub-optimal outcomes. Power control during CBF has not been intricately addressed in current literature. In this paper, a novel approach towards concurrent beamsteering, generalized sidelobe minimization and node transmission power reduction is proposed. The proposed scheme simultaneously adjusts collaborating nodes' transmission phase and amplitude to ensure the intended multiple objectives are met. Firefly Algorithm (FA) is utilized in optimizing the nodes' transmission phase and amplitude. Performance comparisons have been carried out against a scheme featuring concurrent beamsteering and generalized sidelobe minimization only (without node transmission power control). The overall performance has been validated against a peak sidelobe minimization approach (as per the current literature). The proposed scheme is noted to improve node transmission power and overall sidelobe performance whilst maintaining appreciable beamsteering accuracy.

Keywords—Wireless Sensor Network, Collaborative Beamforming, Sidelobes, Firefly Algorithm

I. INTRODUCTION

Wireless sensor networks (WSNs) are progressively being applied in a variety of applications such as environment and climate monitoring, smart medicine, surveillance systems among others [1]–[3]. Most areas of application entail use of low-power sensor nodes featuring elementary hardware. The nodes are usually deployed over a remote area to gather data from the intended immediate environment and forward the same to far-off data sinks/ Base Stations/ Access Points (BSs/APs). Noteworthy, data communication challenges in WSNs are unique from those associated with traditional wireless ad-hoc networks [4], [5]. Appropriate communication protocols/ schemes for WSNs ought to overcome the aspect of limited transmission range associated with individual sensor nodes. Furthermore, node power consumption and processing capacity issues have to be taken into consideration as significant constraints in the design of WSNs communication schemes.

A worthwhile solution to the aforementioned issues is the utilization of the usual high density deployment of sensor nodes to perform Collaborative Beamforming (CBF) in the uplink [6]. Collaborative beamforming entails use of a cluster of sensor nodes to jointly and coherently transmit sensor data to an AP. The cluster of sensor nodes acts as a distributed and random antenna array. The phase of the carriers of the collaborating nodes are adjusted with the intention of realizing a radiation beam directed towards the intended AP. Collaborative beamforming inherently extends sensor nodes' transmission range. Reference can be made to [7], [8].

An outcome of CBF is the presence of uncontrolled sidelobes in the radiation pattern owing to random sensor node locations [9]. Although a CBF beampattern has a deterministic mainlobe (independent of the random sensor node locations), the sidelobes are random/ non-deterministic. Sidelobes are bound to result in high interference at unintended APs. Research in sidelobe minimization in CBF is of utmost necessity. Lower interference at unintended APs through sidelobe minimization inherently increases WSN communication capacity. In respect to limited energy resources at sensor nodes, it is of paramount importance to ensure node transmission power in a CBF process is kept at a low.

The authors in [10] utilize a Canonical Swarm Optimization (CPSO) algorithm to synthesize virtual antenna arrays from randomly deployed sensors in the realm of CBF with the aim of optimizing the mainlobe, sidelobe level and nulls in specific directions. Appreciable results are obtained with sidelobe suppression ranging from 3dB to 15dB. Matters to do with node transmission power control are not explicitly dealt with in the paper. In [11] node selection has been proposed as mechanism for solving the CBF sidelobe control in the context of WSNs. An efficient algorithm with low overhead has been developed and analyzed. Despite achieving comparatively good results, the proposed mechanism is only applicable in high density WSNs. The authors in [12] propose a node selection procedure in the form of a concentric circular ring array using a novel swarm intelligence optimization algorithm Cuckoo Search Chicken Swarm Optimization (CSCSO) to achieve sidelobe minimization in WSNs. To allow for optimal selection of nodes to yield a circular ring array, high node density is a major requirement; this restricts the possible domains of application of the proposed procedure. In [13],

Mr. Robert Macharia Maina, Department of Telecommunication and Information Engineering, JKUAT (e-mail: robertisaacm@gmail.com).
Dr. Kibet Lang'at, Department of Telecommunication and Information Engineering, JKUAT.
Dr. P. K. Kihato, Department of Electrical and Electronic Engineering, JKUAT.

a sidelobe reduction and capacity improvement mechanism in WSNs is presented from the perspective of open-loop collaborative beamforming. Collaborating nodes' transmit amplitude perturbation is utilized towards achieving sidelobe control after a conventional beamsteering procedure. The presented work is in the domain of planar WSN arrangement.

In general, the following shortcomings have been noted:

- The reviewed literature mainly dwells on node selection as the basis of sidelobe control (implying a high node density requirement for successful implementation).
- Sidelobe control is commonly implemented upon conventional beamsteering, with a concentration on peak sidelobe control.
- Node transmission power control during CBF has not been intricately addressed in current literature.
- The area of concentration is in planar WSN configuration.

In this paper, an approach towards concurrent beamsteering, sidelobe minimization and node transmission power reduction is proposed. The new contributions covered in the paper are:

- Design and analysis of a concurrent beamsteering, generalized sidelobe minimization and node transmission power reduction scheme.
- Moreover, the scheme mentioned in 1. is designed and analyzed on the basis of a 3-dimension WSN arrangement as opposed to the commonly utilized CBF platform: a planar WSN configuration.

The rest of the paper is structured as follows. A review of the Firefly Algorithm (FA) is presented in Section II. The proposed beamsteering, sidelobe minimization and node transmission power reduction model is presented in Section III. The performance of the proposed technique is analyzed in Section IV.

II. FIREFLY ALGORITHM

The Firefly Algorithm (FA) is a swarm-based metaheuristic algorithm with a basis on the manner in which fireflies interact using their flashing lights. The FA makes an assumption that all fireflies are unisex (with the implication that any firefly can be attracted by any other firefly). The attractiveness factor of a firefly is directly proportional to its brightness. The attractiveness/ brightness is mapped onto the objective function under consideration.

Given a ray of light passing through a medium with a light absorption coefficient γ, the light intensity at a distance r from the source is as per (1).

$$I = I_0 \exp^{-\gamma r^2} \tag{1}$$

where I_0 is the light intensity at the source.

On the basis of (1), a generalized brightness function is modelled as per (2).

$$\beta = \beta_0 \exp^{-\gamma r^\omega} \tag{2}$$

where β_0 is the brightness at the source and $\omega \geq 1$

In the case of a minimization problem, a solution (*firefly*) corresponding to the smallest objective function value is assigned the highest brightness. Other *fireflies* are more or less attracted to the brightest firefly in a manner depicted in (3).

$$x_{i+1} = x_i + \beta_0 \exp^{-\gamma r_{ij}^\omega}(x_j - x_i) + \alpha\varepsilon \tag{3}$$

where x is a firefly position vector, j is representative of the brightest firefly, i a less bright firefly, α is a step constant and ε is a random vector in the range $0 \rightarrow 1$.

The position of the brightest firefly is perturbed as per (4)

$$x_{j+1} = x_j + \alpha\varepsilon \tag{4}$$

Reference can be made to [14]–[16].

III. METHODOLOGY

The adopted WSN node arrangement is as per Fig. 1. The sensor nodes and the data sink (access point) are configured in a random 3-dimension manner. As far as the nodes' transmitting antennas are concerned, the arrangement is akin to a non-uniform 3-dimension array.

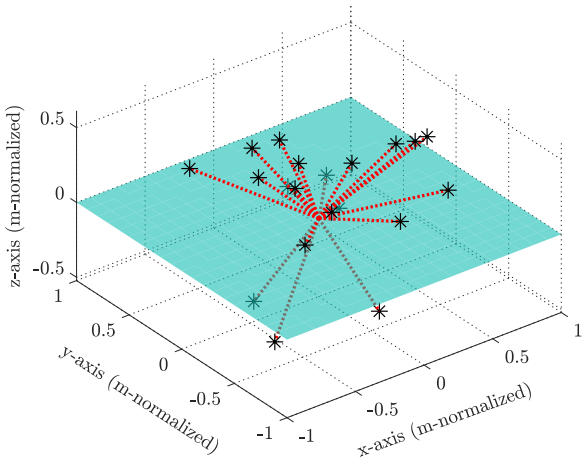

Fig. 1. utilized node arrangement (normalized scale).

The array factor corresponding to the arrangement is as per (5).

$$AF_{\phi,\theta} \approx \sum_{q=1}^{Q} w_q e^{j\frac{2\pi}{\lambda}[\mathbf{R}_q \cdot \mathbf{e}_r]} \tag{5}$$

where $AF_{\phi,\theta}$ is the array factor in direction (ϕ, θ), ϕ is the azimuth angle and θ is the elevation angle, w_q is the q^{th} sensor node transmit weighting, $\mathbf{R}_q$ is the position of the q^{th} sensor node with reference to the collaborating nodes' cluster head, $\mathbf{e}_r = \sin(\theta)\cos(\phi)\mathbf{a}_x + \sin(\theta)\sin(\phi)\mathbf{a}_y + \cos(\theta)\mathbf{a}_z$.

Sidelobe minimization is achieved though optimizing the expression given in (6) with the complex node weights as the function variables.

$$\text{minimize} \qquad \frac{\sum_{SL} |AF_{\phi_{SL},\theta_{SL}}(\mathbf{w})|^2}{M_{SL}} \tag{6}$$

where M_{SL} is the number of all sidelobes, (ϕ_{SL}, θ_{SL}) are sidelobe directions and $(\mathbf{w})$ is the node transmit weights vector.

Transmit power control is achieved though optimizing the expression given in (7).

$$\text{minimize} \qquad \sum_{q} |w_q|^2 \tag{7}$$

$|w_q|$ is the amplitude of the q^{th} sensor node transmit weighting.

Beamsteering is achieved though maximizing the expression given in (8) with the complex node weights as the function variables.

$$\text{maximize} \qquad |AF_{\phi_d,\theta_d}(\mathbf{w})|^2 \tag{8}$$

where (ϕ_d, θ_d) is the beamsteering direction.

The overall objective function (beamsteering + sidelobe minimization + power control) is framed as linear combination of (6), (7) and (8) as per (9).

$$\text{minimize} \quad -|AF_{\phi_d,\theta_d}(\mathbf{w})|^2 + \frac{\sum_{SL} |AF_{\phi_{SL},\theta_{SL}}(\mathbf{w})|^2}{M_{SL}} + \sum_{q} |w_q|^2 \tag{9}$$

The objective function corresponding to beamsteering and sidelobe minimization without power control is as per (10).

$$\text{minimize} \qquad -|AF_{\phi_d,\theta_d}(\mathbf{w})|^2 + \frac{\sum_{SL} |AF_{\phi_{SL},\theta_{SL}}(\mathbf{w})|^2}{M_{SL}} \tag{10}$$

The overall performance of the proposed CBF scheme as per equation (9) has been validated against a peak sidelobe minimization scheme as per (11).

$$\text{minimize} \qquad -|AF_{\phi_d,\theta_d}(\mathbf{w})|^2 + |AF_{\phi_{PeakSL},\theta_{PeakSL}}(\mathbf{w})|^2 \tag{11}$$

where $(\phi_{PeakSL}, \theta_{PeakSL})$ is the direction of the peak sidelobe.

The selected beamsteering direction is $(\phi_d, \theta_d) \Rightarrow (80 \text{ degrees}, 40 \text{ degrees})$.

The FA algorithm is utilized in optimizing (9), (10) and (11). The FA algorithm is run over a total of 60 iterations. To allow for fair comparison given that the FA algorithm is stochastic in nature, results are generated from 100 independent optimization runs.

IV. RESULTS AND DISCUSSION

The focus of the results analysis process is in the nature of the obtained radiation patterns and the relative node transmission weights. The radiation patterns presented herein are representative of the average outcome of 100 independent optimization runs.

The relative radiation patterns (in the form of contour plots) corresponding to optimizing (9) and (10) are as per Figs. 2 and 3 respectively. Fig. 2 is representative of the resultant radiation pattern with node transmission power control. Fig. 3 is representative of the resultant radiation pattern without node transmission power control. As per the two radiation patterns, radiation power is concentrated in the desired direction. Qualitatively, there are no observable differences between the plots.

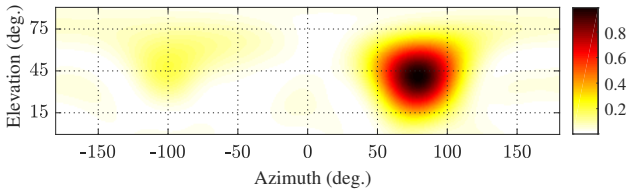

Fig. 2. Radiation pattern in contour plot form (with node transmission power control).

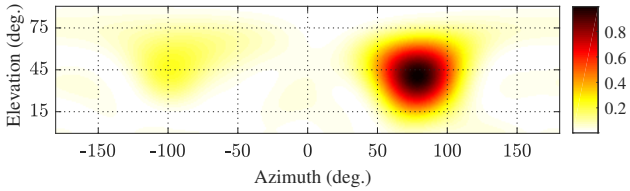

Fig. 3. Radiation pattern in contour plot form (without node transmission power control).

The relative radiation patterns (in the form of mesh plots) corresponding to optimizing (9) and (10) are as per Figs. 4 and 5 respectively. Fig. 4 is representative of the resultant radiation pattern with node transmission power control. Fig. 5 is representative of the resultant radiation pattern without node transmission power control. The patterns are relatively similar with radiation power mainly concentrated in the desired direction.

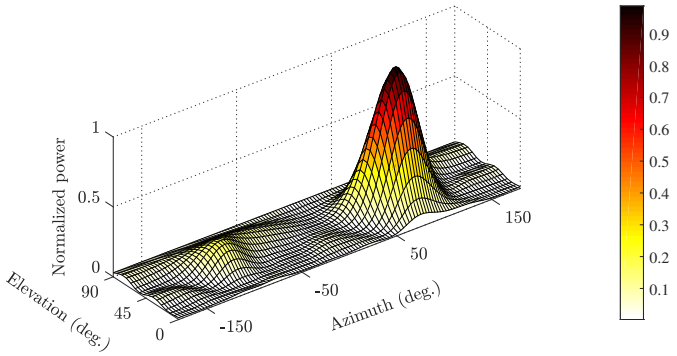

Fig. 4. Radiation pattern in mesh plot form (with node transmission power control).

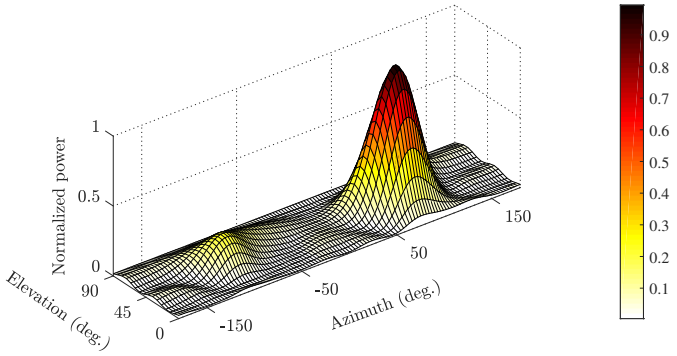

Fig. 5. Radiation pattern in mesh plot form (without node transmission power control).

As per the presented radiation pattern plots (in the form of contour and mesh plots), introduction of power control in CBF does not hamper the overall radiation performance.

Figs. 6 and 7 depict azimuthal (in the beamsteering elevation plane) radiation pattern comparison plots in normalized form. Fig. 6 is at a raw scale and Fig. 7 is at a decibel scale. It is noteworthy that the radiation pattern corresponding to the power control mechanism has slightly lower sidelobes, an aspect that is more pronounced in Fig. 7.

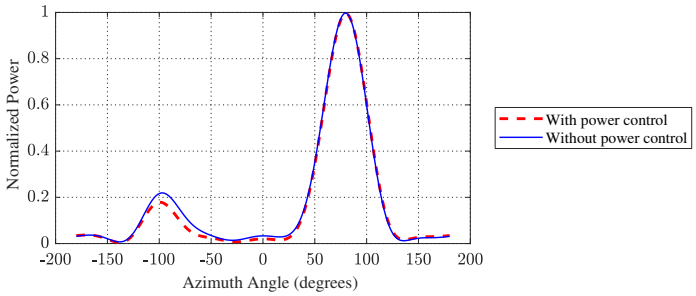

Fig. 6. An azimuth cut of the normalized radiation pattern: at the beamsteering elevation angle (40 degrees).

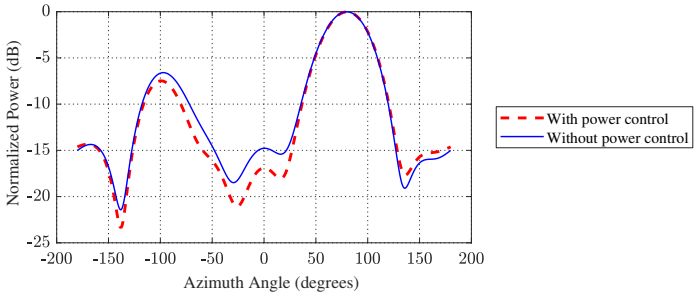

Fig. 7. An azimuth cut of the normalized radiation pattern in a decibel scale: at the beamsteering elevation angle (40 degrees).

Figs. 8 and 9 depict elevation (in the beamsteering azimuth plane) radiation pattern comparison plots in normalized form. Qualitatively, the radiation pattern plots are nearly identical.

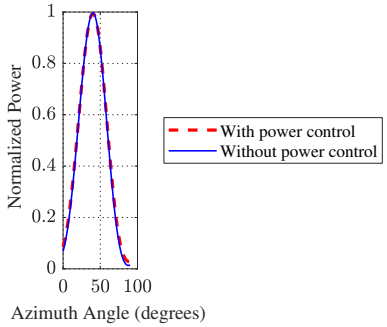

Fig. 8. An elevation cut of the normalized radiation pattern: at the beamsteering azimuth angle (80 degrees).

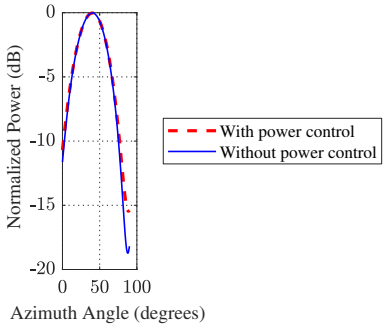

Fig. 9. An elevation cut of the normalized radiation pattern in a decibel scale: at the beamsteering azimuth angle (80 degrees).

The presented azimuth and elevation cut radiation pattern plots imply that the application of the proposed power control scheme in CBF does not hamper the overall radiation performance and is bound to result in better radiation characteristics (as noted in the azimuth cut plots).

A quantitative comparison in terms of radiation pattern data is given in Table I. The data encompasses normalized radiation power in the desired and undesired directions. The presented data is the average outcome of 100 independent optimization runs.

TABLE I
RADIATION PATTERN DATA. BEAMSTEERING WITH: GENERALIZED SIDELOBE MINIMIZATION WITH/ WITHOUT POWER CONTROL; PEAK SIDELOBE MINIMIZATION.

	With PC.		Without PC		PSL min.	
	Mean	SD	Mean	SD	Mean	SD
Norm. power in desired dir.	0.993	0.005	0.991	0.014	0.994	0.007
Norm. power in undesired dir.	0.081	0.003	0.082	0.005	0.093	0.009

Analysis of variance (ANOVA) test on the *normalized power in the desired direction* data as per Table I yields the outcome given in Table II.

TABLE II
ANOVA TEST OUTCOME ON THE NORMALIZED POWER DIRECTED TOWARDS THE DESIRED DIRECTION.

Source	Sum of Squares	df	Mean Squares	F	P
Between	0.000467	2	0.000233	2.626461	0.074014
Within	0.026385	297	0.000089		
Total	0.026852	299	0.000090		

The obtained P value (> 0.05) is indicative of absence of any significant differences between the means of the *normalized power in the desired direction* data. The 3 schemes yield statistically identical beamsteering accuracy/ capability. In essence, use of the proposed *generalized sidelobe minimization* rather than the commonly utilized *peak sidelobe minimization* does not hamper beamsteering accuracy/ capability.

An ANOVA test on the *normalized power in the undesired directions* data as per Table I yields the outcome given in Table III.

TABLE III
ANOVA TEST OUTCOME ON THE NORMALIZED POWER DIRECTED TOWARDS THE UNDESIRED DIRECTIONS.

Source	Sum of Squares	df	Mean Squares	F	P
Between	0.008867	2	0.004433	115.652174	7.1785E-38
Within	0.011385	297	0.000038		
Total	0.020252	299	0.000068		

The obtained P value (< 0.05) is indicative of a significant difference between the means of the *normalized power in the undesired directions* data. The difference(s) are as per the outcome of a Tukey-Kramer test as given in Table IV where:

- GSLmPC: Beamsteering with generalized sidelobe minimization and power control.
- GSLm: Beamsteering with generalized sidelobe minimization only (without power control).
- PSLm: Beamsteering with peak sidelobe minimization only.

TABLE IV
TUKEY-KRAMER COMPARISON TEST ON THE NORMALIZED POWER DIRECTED TOWARDS THE UNDESIRED DIRECTIONS.

Comparison	Absolute Difference	Std. Error of Difference	Critical Range	Results
GSLmPC/ GSLm	0.001	0.00061914	0.0024	Equivalent means
GSLmPC/ PSLm	0.012		0.0024	Different means
GSLm/ PSLm	0.011		0.0024	Different means

Statistically, the CBF scheme featuring generalized sidelobe minimization with power control yields an *undesired radiation power* outcome identical to that of the scheme featuring generalized sidelobe minimization only. The two generalized sidelobe minimization schemes outperform the peak sidelobe minimization only scheme (in terms of *undesired radiation power*).

Typical node weights obtained in the CBF processes are given in Table V. The node weights presented in Table V are graphically compared in Fig. 10. The presented results are a snapshot of one of the independent 100 optimization runs. There is a reduction in the average node transmission weight amplitude upon utilizing power control in the CBF process. This is over and above the fact that the power control mechanism does not hamper the concentration of radiation power towards the desired direction.

TABLE V
NODE WEIGHTS UPON CBF (FEATURING SIDELOBE MINIMIZATION) WITH POWER CONTROL AND WITHOUT POWER CONTROL.

	With power control		Without power control	
Node	Amplitude	Phase	Amplitude	Phase
1	1	66.9	1	171.27
2	1	15.02	1	105.12
3	1	-138.48	1	-43.42
4	0.98	-23.54	0.78	77.42
5	0.98	-23.77	1	63.32
6	1	92.36	1	-177.82
7	0.99	100.21	0.99	166.21
8	0.87	-1.02	1	102.64
9	0.98	-83.14	1	88.63
10	1	82.44	1	175.71
11	0.31	12.58	0.97	107.06
12	0.99	-69.89	0.85	27.84
13	0.64	-176.05	1	-62.72
14	0.99	178.69	1	-85.59
15	1	77.41	0.96	-171.83
16	1	99.74	1	166.49
17	1	-86.82	0.99	4.74
18	0.84	-29.54	1	72.03
19	0.91	-78.81	0.95	-13.52
20	0.92	11.58	0.93	86.47
Average	0.92		0.971	
Maximum	1		1	
Minimum	0.31		0.78	
Total	18.4		19.42	
Normalized power in the look direction (as per the Rad. pattern)	*0.993*		*0.991*	

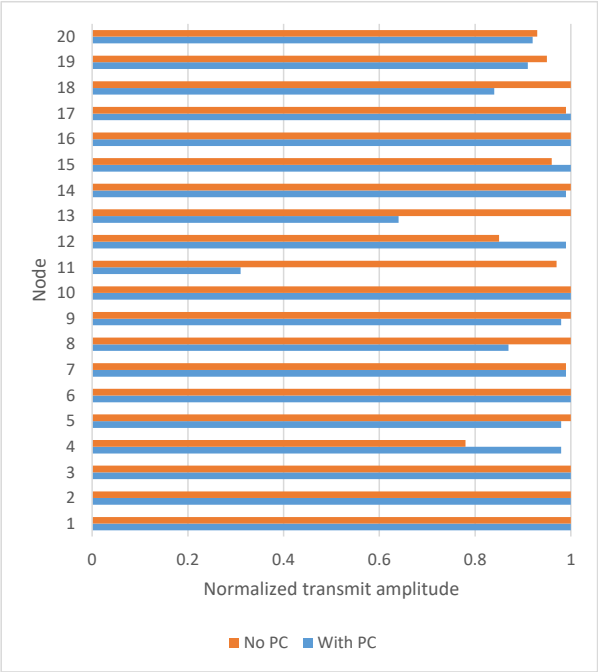

Fig. 10. Normalized transmit amplitudes at collaborating nodes upon CBF (featuring sidelobe minimization) with power control and without power control.

V. CONCLUSION

This paper has presented the design and analysis of a novel mechanism geared towards simultaneous beamsteering, sidelobe control and transmission power control in the domain of CBF in WSNs. The multi-objective CBF criterion has been optimized using the FA algorithm. A comparative analysis has been made against a beamsteering and sidelobe control mechanism (without power control). It has been established that introduction of transmission power control generally leads to better CBF performance. Lower node transmission power is the general outcome, without hampering the relative radiation strength in the desired direction and the average sidelobe level/ radiation in undesired directions. Noteworthy, the proposed CBF scheme has been implemented and analyzed on the basis of a 3-dimension WSN arrangement, a new approach in comparison to the commonly utilized 2-dimension WSN arrangement.

REFERENCES

[1] D. Kandris, C. Nakas, D. Vomvas, and G. Koulouras, "Applications of wireless sensor networks: an up-to-date survey," *Applied System Innovation*, vol. 3, no. 1, p. 14, 2020.

[2] R. Kashyap, "Applications of wireless sensor networks in healthcare," in *IoT and WSN Applications for Modern Agricultural Advancements: Emerging Research and Opportunities*, pp. 8–40, IGI Global, 2020.

[3] P. Rupa, S. Singh, S. Arvind, and P. Johri, "A comprehensive survey on applications of wireless sensor networks and approaches to control congestion," *ICDSMLA 2019*, pp. 805–812, 2020.

[4] B. Bhushan and G. Sahoo, "Requirements, protocols, and security challenges in wireless sensor networks: An industrial perspective," in *Handbook of computer networks and cyber security*, pp. 683–713, Springer, 2020.

[5] P. K. Singh and M. Paprzycki, "Introduction on wireless sensor networks issues and challenges in current era," in *Handbook of Wireless Sensor Networks: Issues and Challenges in Current Scenario's*, pp. 3–12, Springer, 2020.

[6] L. Shi, Z. Li, X. Ding, J. Xu, and Z. Lv, "Optimizing wireless sensor networks based on collaborative beamforming," *Procedia Computer Science*, vol. 174, pp. 561–571, 2020.

[7] S. Felici-Castell, E. A. Navarro, J. J. Pérez-Solano, J. Segura-García, and M. García-Pineda, "Practical considerations in the implementation of collaborative beamforming on wireless sensor networks," *Sensors*, vol. 17, no. 2, p. 237, 2017.

[8] S. Jayaprakasam, S. K. A. Rahim, and C. Y. Leow, "Distributed and collaborative beamforming in wireless sensor networks: Classifications, trends, and research directions," *IEEE Communications Surveys & Tutorials*, vol. 19, no. 4, pp. 2092–2116, 2017.

[9] S. Liang, Z. Fang, G. Sun, Y. Liu, G. Qu, and Y. Zhang, "Sidelobe reductions of antenna arrays via an improved chicken swarm optimization approach," *IEEE Access*, vol. 8, pp. 37664–37683, 2020.

[10] M. Z. Hasan and H. Al-Rizzo, "Beamforming optimization in internet of things applications using robust swarm algorithm in conjunction with connectable and collaborative sensors," *Sensors*, vol. 20, no. 7, p. 2048, 2020.

[11] G. Sun, Y. Liu, Z. Chen, A. Wang, Y. Zhang, D. Tian, and V. C. Leung, "Energy efficient collaborative beamforming for reducing sidelobe in wireless sensor networks," *IEEE Transactions on Mobile Computing*, 2019.

[12] G. Sun, Y. Liu, S. Liang, Z. Chen, A. Wang, Q. Ju, and Y. Zhang, "A sidelobe and energy optimization array node selection algorithm for collaborative beamforming in wireless sensor networks," *IEEE Access*, vol. 6, pp. 2515–2530, 2017.

[13] S. Jayaprakasam, S. K. Abdul Rahim, C. Y. Leow, and T. O. Ting, "Sidelobe reduction and capacity improvement of open-loop collaborative beamforming in wireless sensor networks," *PloS one*, vol. 12, no. 5, p. e0175510, 2017.

[14] V. Kumar and D. Kumar, "A systematic review on firefly algorithm: past, present, and future," *Archives of Computational Methods in Engineering*, vol. 28, no. 4, pp. 3269–3291, 2021.

[15] H. Wang, W. Wang, H. Sun, and S. Rahnamayan, "Firefly algorithm with random attraction," *International Journal of Bio-Inspired Computation*, vol. 8, no. 1, pp. 33–41, 2016.

[16] H. Wang, W. Wang, X. Zhou, H. Sun, J. Zhao, X. Yu, and Z. Cui, "Firefly algorithm with neighborhood attraction," *Information Sciences*, vol. 382, pp. 374–387, 2017.